



Article

Effect of Osmolytes on Photoassembly of Functionally Active Mn_4CaO_5 Cluster in Mn-Depleted Photosystem II Preparations Isolated from Spinach Leaves

Denis V. Yanykin ^{1,2,*} , Dina V. Kazantseva ¹ and Andrey A. Khorobrykh ²

¹ Prokhorov General Physics Institute of the Russian Academy of Sciences, 38 Vavilova St., Moscow 119991, Russia; dinacazantsewa@yandex.ru

² Institute of Basic Biological Problems, FRC PSCBR, Russian Academy of Sciences, 2 Institutskaya St., Pushchino 142290, Russia; andrewkhor@rambler.ru

* Correspondence: ya-d-ozh@rambler.ru

Abstract: The effect of osmolytes (trehalose, sucrose, betaine, D-glucose and hydroxyectoine) on the photoassembly of the functionally active inorganic core of the water-oxidizing complex (Mn_4CaO_5 cluster) in Mn-depleted PSII preparations (apo-WOC-PSII) was investigated. It was revealed that the efficiency of the photoassembly of the Mn_4CaO_5 cluster was considerably (three times) increased in the presence of 1 M disaccharides (trehalose or sucrose) in contrast to other osmolytes. It was found that the osmolytes (especially trehalose or sucrose) improved the redox interaction of exogenous Mn^{2+} with apo-WOC-PSII, enhanced the protective effect of Mn^{2+} against the photoinhibition of apo-WOC-PSII, protected $CaCl_2$ -treated PSII preparations against thermoinactivation, and stabilized the water-oxidizing complex and electron transport from Q_A to Q_B in native PSII preparations during heat treatment. It is suggested that the ability of osmolytes to enhance the efficiency of the photoassembly of a Mn_4CaO_5 cluster depends on their effect on the following key processes: the redox interaction of Mn^{2+} with apo-WOC-PSII; the stability of apo-WOC-PSII to photoinhibition during the photoactivation procedure; and the stabilization of both the newly assembled functionally active Mn_4CaO_5 cluster and the electron transfer from Q_A to Q_B .

Keywords: photosystem II; water-oxidizing complex; photoassembly of Mn_4CaO_5 cluster; osmolytes; photosynthetic electron transfer



Citation: Yanykin, D.V.; Kazantseva, D.V.; Khorobrykh, A.A. Effect of Osmolytes on Photoassembly of Functionally Active Mn_4CaO_5 Cluster in Mn-Depleted Photosystem II Preparations Isolated from Spinach Leaves. *Horticulturae* **2023**, *9*, 1339. <https://doi.org/10.3390/horticulturae9121339>

Academic Editors:

Sara González-Orenga, M.
Iftikhar Hussain and
Muhammad Ikram

Received: 10 November 2023

Revised: 6 December 2023

Accepted: 13 December 2023

Published: 14 December 2023



Copyright: © 2023 by the authors. Licensee MDPI, Basel, Switzerland. This article is an open access article distributed under the terms and conditions of the Creative Commons Attribution (CC BY) license (<https://creativecommons.org/licenses/by/4.0/>).

1. Introduction

Photosystem II (PSII) is a pigment–protein complex located in the thylakoid membrane. PSII catalyzes the light-induced oxidation of water to O_2 and the reduction of plastoquinone. The photochemical reaction center (RC) of PSII converts the excitation energy of chlorophyll into the energy of separated charges and produces the strongest biological oxidant, a dimer of chlorophyll *a* designated as $P_{680}^{+\bullet}$, with a redox potential of 1.1–1.27 V [1–3]. To oxidize water, the water-oxidizing complex (WOC) containing an enzymatic center with the inorganic core (Mn_4CaO_5 cluster) is oxidized via the sequential absorption of photons and charge separation in the RC to form a series of intermediate states called S-states (S_0 , S_1 , S_2 , S_3 and S_4), with the transition from S_4 to S_0 accompanied by the oxidation of two molecules of water and the production of O_2 .

Leaves absorb light energy, which can damage the photosynthetic apparatus and lead to photoinhibition. The development of photoinhibition depends on environmental conditions such as water stress and temperature [4–9]. PSII is especially sensitive to photoinhibition [10]. Photoinhibition leads ultimately to the degradation of the D1 protein, which is synthesized in vivo and re-built into the PSII (see reviews [11,12]). So, PSII repair includes the replacement of a damaged D1 protein with a newly synthesized D1. Since the majority of the ligands of the Mn_4CaO_5 cluster are located on the D1 protein, the

photoassembly of the inorganic core of the WOC is also required after the replacement of the damaged D1 protein with a new one. The process of photoassembly of Mn_4CaO_5 cluster is called the photoactivation of PSII. Briefly, the photoassembly of the Mn_4CaO_5 cluster can be described by the following steps: photooxidation of the first bound Mn^{2+} to Mn^{3+} and then formation of a $\text{Mn}^{3+}\text{--Mn}^{2+}$ complex. The following light-induced charge separation in the RC leads to the oxidation of this complex with the formation of a metastable $\text{Mn}^{3+}\text{--Mn}^{3+}$ complex. The coordination of two other Mn^{2+} ions (which are also oxidized) leads to the formation of a functionally active Mn_4CaO_5 cluster. This kinetic model has been designated as a “two-quantum series model” [13]. The molecular mechanisms that cause these kinetic features remain unresolved.

The experiments on the photoassembly of the Mn_4CaO_5 cluster were mainly carried out on isolated PSII membranes lacking a Mn_4CaO_5 cluster. Although the photoassembly of the Mn_4CaO_5 cluster in these cases may be different from that in vivo, in vitro studies provided a wide range of information regarding the cofactors involved in the photoassembly of the Mn_4CaO_5 cluster [14–27]. A detailed description of the PSII photoactivation is presented in the reviews in [28–30]. It is known that the donor side of PSII is selectively inactivated under the illumination of a PSII-deprived Mn_4CaO_5 cluster, and the damage to PSII components is ascribed to the formation of the long-lived forms of $\text{P}_{680}^{+\bullet}$ or TyrZ^\bullet [31–34]. So, the photoactivation of oxygen-evolving activity in apo-WOC-PSII preparations is carried out with low-intensity light and at high concentrations of Mn^{2+} ions to exclude the formation of the long-lived forms of $\text{P}_{680}^{+\bullet}$ or TyrZ^\bullet . In addition to the light-induced oxidation of Mn^{2+} ions, the stabilization of an assembled functionally active Mn_4CaO_5 cluster seems to be required.

Plants often produce osmolytes, which are membrane-impermeable solutes that accumulate in the cytoplasm to very high concentrations [35]. One of the best-known and important mechanisms of abiotic stress response adopted by plants is the biosynthesis and accumulation of osmolytes. Osmolytes remain non-toxic, even at molar concentrations. The most common osmolytes include sugars (trehalose and sucrose), amino acids (proline, glutamate, glutamine and alanine) and their derivatives (ectoine and hydroxyectoine), quaternary amines (betaine, polyamines and dimethyl sulfoniopropionate) and polyols including sugar alcohols (mannitol, sorbitol, pinitol, glycerol and galactinol) [36–38].

These osmoprotectors perform many functions during stress events, including the scavenging of ROS; balancing cell redox; and the stabilization of pH, proteins, enzymes and membranes [38–41]. The accumulation of sucrose [42], trehalose [43] and raffinose [44] is observed in dehydrating resurrection plants. Saccharides (such as sucrose) are known membrane protectants that can stabilize cellular processes [45]. It is known that glucose and sucrose accumulate in specific locations in resurrection plant tissue during dehydration and probably function to protect specific cellular structures (e.g., chloroplasts and tonoplast membranes) from desiccation [46]. Sugars, such as trehalose, are involved in preventing protein aggregation during desiccation [47]. Unlike other sugars, trehalose is distinguished by its unique physicochemical properties such as inertness, thermal stability, high glass transition temperature, and stability over a wide pH range [48–51]. Studies of trehalose effect on biological objects found that trehalose increases the resistance of plants to drought and salinization [52–54], the action of heavy metals [55], and the effects of low [56] and high [57] temperatures.

It is known that different osmolytes can stabilize the PSII complex, which is the most sensitive component of the photosynthetic membrane to the action of various stress factors (temperature and light) [58–64], and also increases the PSII photochemical activity [65]. It was shown that betaine stabilizes the WOC during the incubation of PSII membranes at room temperature, alkaline pH and high salt concentrations by preventing the dissociation of extrinsic proteins and manganese ions from the WOC [58,61,66,67]. It was shown that partial electron transfer reactions that are more intimate with the reaction center complex are also stabilized by glycinebetaine and sucrose [61]. Another osmolyte, hydroxyectoine, is among the most studied osmolytes in relation to the stabilization of biomolecules. Recently, it was shown that hydroxyectoine stimulates the oxygen-evolving activity of PSII and

enhances the protective effect of exogenous electron donors against the donor-side photoinhibition of apo-WOC-PSII preparations [68]. One of the carbohydrates that stand out among others is trehalose. It was shown that trehalose protects PSII during thawing [69,70] and prevents the aggregation and inactivation of PSII membrane fragments during long-term storage [71], although it does not exhibit a protective effect during the thermal inactivation of isolated PSII D1/D2/cyt b_{559} reaction center complexes of PSII [62]. It has been demonstrated that the addition of trehalose stabilizes electron transport in oxygen-evolving PSII preparations [72,73]. In addition to the protective properties, trehalose acts on electronic transport in bacterial type 2 reaction centers [74] and apo-WOC-PSII [75]. It has been shown that the Mn^{2+} -induced protection of apo-WOC-PSII against photoinactivation is greatly increased in the presence of trehalose [64]. It may indicate that trehalose reorganizes the donor side of apo-WOC-PSII, and that, in turn, contributes to better electron transfer from Mn^{2+} to RC of PSII. Trehalose increases the rate of oxygen evolution in PSII core complexes and PSII membrane fragments [71] that, according to the author's assumption, is associated with the transition of PSII to a more optimal conformation caused by changes in the hydration of PSII. In addition, the investigation of the protein dynamics associated with the $S_1 \rightarrow S_2$ transition of WOC in PSII core complexes by the use of FTIR spectroscopy in the presence of a substrate-based inhibitor, ammonia, allowed for trehalose to exclude water molecules from the solvation layer of the WOC [76]. However, later, additional data disproved this hypothesis while strongly supporting the water entrapment and anchorage models [77]. Moreover, the addition of trehalose induces the transformation of Q_B -non-reducing PSII RC into Q_B -reducing PSII RC [75], which decreased the probability of charge recombination in RCs.

In this work, we investigate the effect of osmolytes sucrose, trehalose, betaine, D-glucose and hydroxyectoine (Ect-OH) on the restoration of oxygen-evolving activity in the apo-WOC-PSII related to the photoassembly of the functionally active Mn_4CaO_5 cluster.

2. Materials and Methods

2.1. Isolation and Treatment of PSII Preparations

Spinach plants were grown in a greenhouse (Institute of Basic Biological Problems, FRC PSCBR, Russian Academy of Sciences, Pushchino, Russia) at a temperature of 20/15 °C (day/night) and under natural illumination from 20 February 2023 to 25 April 2023. Oxygen-evolving PSII membranes were isolated from spinach leaves [78]. The preparations were suspended (2 mg Chl/mL) in a medium containing 50 mM Mes-NaOH (pH 6.5), 35 mM NaCl, 0.33 M sucrose and 10% glycerol and stored at -76 °C. The concentration of chlorophyll was determined as described previously [79]. PSII membranes deprived of the Mn cluster (apo-WOC-PSII) were obtained by NH_2OH treatment as described previously [15]. In order to obtain PSII preparations with WOC-depleted extrinsic proteins without the extraction of a Mn_4CaO_5 cluster from the WOC. The oxygen-evolving PSII preparations were treated by 1 M $CaCl_2$ ($CaCl_2$ -PSII preparations) [80]. In order to obtain PSII preparations with the two WOC-depleted extrinsic proteins PsbP and PsbQ without the removal of the PsbO protein and the Mn cluster, the oxygen-evolving PSII preparations were treated with 1 M NaCl (NaCl-PSII preparations) [81].

2.2. Procedure for Photoassembly of Functionally Active Mn_4CaO_5 Cluster in apo-WOC-PSII Preparations and Measurement of Oxygen-Evolving Activity

The photoassembly of functionally active Mn_4CaO_5 cluster in apo-WOC-PSII preparations was performed at 25 °C at a Chl concentration of 200 μg Chl/mL in the medium containing 50 mM Mes-NaOH (pH 6.5), 35 mM NaCl, $MnCl_2$ (0.01–1 mM), 50 mM $CaCl_2$ and 50 μM DCP/IP in the absence or in the presence of 1 M osmolytes. After that, the apo-WOC-PSII preparations were illuminated for a designated time with red light-emitting diodes ($\lambda = 625$ nm, 35 μmol photon $m^{-2} s^{-1}$). The efficiency of the photoassembly of a Mn_4CaO_5 cluster in apo-WOC-PSII preparations was determined based on the ability of the samples to produce photosynthetic oxygen. For all the samples, the rate of light-induced

evolution of O₂ was measured by monitoring the concentration of O₂ with a Clark-type oxygen electrode for 60 s after starting the continuous saturating actinic illumination ($\lambda > 650$ nm, 1500 $\mu\text{mol photon m}^{-2} \text{s}^{-1}$).

To standardize the measurement of oxygen-evolving activity, photoactivated apo-WOC-PSII preparations were diluted ten times with the medium containing 50 mM Mes-NaOH (pH 6.5), 35 mM NaCl, 0.33 M sucrose and 20 mM CaCl₂ to a final concentration of 20 $\mu\text{g Chl/mL}$ (in this case, the concentration of the additions used during photoactivation of the samples decreased 10 times); then, the electron acceptors (1 mM ferricyanide and 100 $\mu\text{M DCBQ}$) were added. In preliminary experiments, it was shown that the addition of any osmolytes in the concentration of 0.1 M to the measurement medium did not affect the oxygen-evolving activity of the photoactivated samples.

2.3. Mn²⁺ Photooxidation in apo-WOC-PSII and Mn-Dependent Protection of apo-WOC-PSII Preparations against Photoinhibition

According to previous publications [82,83], it was shown that the removal of manganese from the WOC led to a significant decrease in photoinduced changes in the yield of chlorophyll *a* fluorescence (F_v) associated with the photoreduction of the primary quinone electron acceptor Q_A. This is due to the loss of electron donation from the WOC to the PSII RC. The addition of Mn²⁺ or another electron donor for PSII restores the electron transport in the PSII reaction center, which causes an increase in photoinduced F_v. Therefore, the efficiency of Mn²⁺ photooxidation in apo-WOC-PSII was determined based on the degree of F_v restoration. The kinetics of F_v were measured in the medium containing 50 mM Mes (pH 6.5) and 35 mM NaCl in the absence of osmolytes or in the presence of 1 M osmolytes at a chlorophyll concentration of 10 $\mu\text{g/mL}$ in a 10 mm cuvette at room temperature using a MULTI-COLOR PAM fluorometer (Waltz, Eichenring, Effeltrich, Germany).

The effect of osmolytes on the Mn-dependent protection of apo-WOC-PSII preparations against photoinhibition was studied as described earlier [64]. The samples were re-suspended at a concentration of 20 $\mu\text{g Chl/mL}$ in a medium containing 50 mM Mes (pH 6.5) and 35 mM NaCl without or with 1 M osmolytes. Then, the samples were illuminated ($\lambda = 625$ nm, 15 $\mu\text{mol photon m}^{-2} \text{s}^{-1}$) in the absence or in the presence of various concentrations of Mn²⁺. After 5 min of illumination, the samples were diluted twice and incubated in the dark for 10 min; then, an electron donor, 2 mM sodium ascorbate, was added, and F_v was measured. The degree of photoinhibition was determined based on the loss of the ability of apo-WOC-PSII preparations to reactivate the F_v with ascorbate. Ascorbate was chosen because its ability to restore F_v did not depend on the presence of osmolytes. The F_v amplitude measured in the apo-WOC-PSII preparations before photoinhibition in the presence of 2 mM sodium ascorbate was taken as 100%.

2.4. Determination of Stability of CaCl₂-PSII Preparations

The stability of CaCl₂-PSII preparations during their incubation at 25 °C was determined based on the loss of oxygen-evolving activity of the samples. The incubation of CaCl₂-PSII preparations was performed in the dark at 110 $\mu\text{g Chl/mL}$ in a medium containing 50 mM Mes (pH 6.5), 35 mM NaCl and 20 mM Ca²⁺ (medium A) in the absence or in the presence of 1 M osmolytes. After that, the preparations were diluted 11 times with medium A containing 0.01 M osmolytes, and then, the electron acceptors (1 mM ferricyanide and 100 $\mu\text{M DCBQ}$) were added. As a result of this dilution, the concentration of osmolytes during the measurement of oxygen-evolving activity was equal to 0.1 M. So, in order for the measurement conditions to be the same, the samples incubated in the absence of osmolyte were diluted with media containing 0.11 M osmolytes.

2.5. Estimation of Heat-Induced Inhibition of Electron Transfer in PSII

The study of the degree of heat-induced inhibition of electron transfer in PSII in the absence and in the presence of osmolytes was studied via fast chlorophyll *a* fluorescence (ChlF) kinetics with a high time resolution using a MULTI-COLOR PAM fluorometer. PSII

preparations with an intact WOC before and after heat treatment were illuminated with saturating 880 ms flashes ($\lambda = 625$ nm, $2360 \mu\text{mol photons m}^{-2} \text{s}^{-1}$), and fluorescence data were recorded.

The heat treatment (incubation of the samples for 40 min at 30°C) was performed in darkness both in the absence and in the presence of the osmolytes in a medium containing 50 mM Mes (pH 6.5) and 35 mM NaCl at $10 \mu\text{g Chl/mL}$. The measurements of the ChlF kinetics were carried out in a medium containing 50 mM Mes (pH 6.5) and 35 mM NaCl at $10 \mu\text{g Chl/mL}$ at room temperature 25°C . The double normalization of ChlF transients between 20 μs and 3 ms ($W_{OJ} = (F_t - F_0)/(F_J - F_0)$) and between 20 μs and 30 ms ($W_{OI} = (F_t - F_0)/(F_I - F_0)$) in combination with the generation of difference kinetics (ΔW_{OJ} and ΔW_{OI} ; “after heat treatment” – “before heat treatment”) allowed for the visualization of so-called K-bands and J-bands, respectively.

2.6. Ultrasonic Interferometry and Refractometry

The stability of PSII preparations with an intact WOC, NaCl-PSII preparations or CaCl_2 -PSII preparations during their incubation at 25°C was determined based on the change in relative velocity of an ultrasound using a fixed-length ultrasonic spectrometer [84]. The preparations were dissolved in a medium containing 50 mM Mes (pH 6.5) and 35 mM NaCl in the absence and in the presence of osmolytes at $200 \mu\text{g Chl/mL}$.

Refractive index measurements were performed using a Multiwavelengths Refractometer Abbemat MW (Anton Paar, Graz, Austria) at 589.3 nm at 25°C .

2.7. Statistical Analysis

In all experiments, data were collected from at least three replicates to ensure reliability of measurements. After data collection, the standard deviation of the measurements was calculated. The presence of the statistically significant differences between experimental groups were tested using one-way analysis of variance (ANOVA), followed by post hoc comparisons by Tukey’s test and Student’s *t*-test for independent means were performed. The normality requirements were checked using Shapiro–Wilk test. The difference was considered significant if $p \leq 0.05$. Origin software was used to carry out these calculations.

3. Results

3.1. Effect of Osmolytes on Photoassembly of Mn_4CaO_5 Cluster in apo-WOC-PSII Preparations

Figure 1 shows the dependence of the efficiency of photoassembly of a Mn_4CaO_5 cluster in apo-WOC-PSII preparations on the duration of the photoactivation procedure. As seen in Figure 1, the efficiency of the photoassembly of a Mn_4CaO_5 cluster increased with increasing exposure of the samples to photoactivating light.

The rate of photosynthetic oxygen evolution in photoactivated PSII preparations after 30 min in the absence of osmolyte was about $17 \mu\text{mol O}_2 (\text{mg Chl h})^{-1}$. The presence of trehalose or sucrose during the photoactivation strongly stimulated the photoassembly so that the rate of oxygen evolution in the samples photoactivated in the presence of the disaccharides reached $55 \mu\text{mol O}_2 (\text{mg Chl h})^{-1}$. Betaine as well as Ect-OH showed weak stimulating effects ($22 \mu\text{mol O}_2 (\text{mg Chl h})^{-1}$). D-glucose, in contrast to other osmolytes, had a negative effect on the photoactivation of the apo-WOC-PSII ($12 \mu\text{mol O}_2 (\text{mg Chl h})^{-1}$). As can be seen, the efficiency of the photoassembly of Mn_4CaO_5 cluster in apo-WOC-PSII was about three times higher in the presence of the disaccharides, while the effect of betaine and Ect-OH was about 30%.

Figure 2 shows the dependence of the photoactivation of apo-WOC-PSII preparations on the concentration of added Mn^{2+} . As previously shown, the maximum yield of the photoactivation of apo-WOC-PSII preparations was observed at 1 mM Mn^{2+} [15] and a further increase in Mn^{2+} concentration led to a decrease in the yield of photoactivation. Thus, the osmolyte effect on the photoassembly of Mn_4CaO_5 cluster was studied within a Mn^{2+} concentration of $10 \mu\text{M}$ to $1000 \mu\text{M}$. The apo-WOC-PSII preparations photoactivated at $10 \mu\text{M Mn}^{2+}$ (corresponding to 10 Mn per reaction center of PSII) showed low rates of

oxygen evolution ($3\text{--}6 \mu\text{mol O}_2 (\text{mg Chl h})^{-1}$) without statistically significant differences between the effects of osmolytes. An increase in the concentration of added Mn^{2+} led to a significant increase in the yield of the photoactivation of apo-WOC-PSII, and the photoactivation was more efficient in the presence of the disaccharides than in the presence of other osmolytes or in their absence (Figure 2).

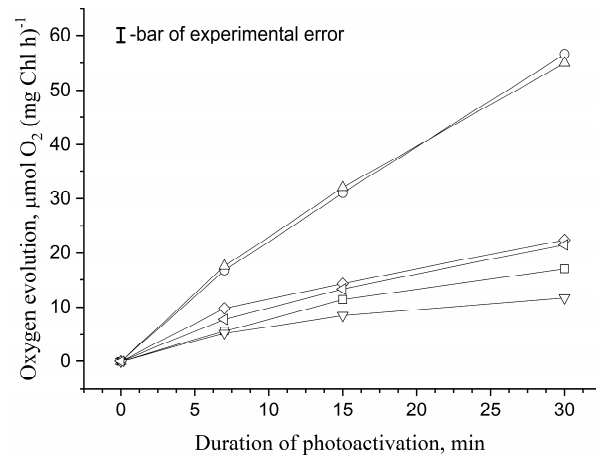


Figure 1. Dependence of the photoactivation of the O_2 -evolving activity in apo-WOC-PSII preparations on duration of photoactivation procedure. The procedure was performed in the absence (\square) and in the presence of 1 M sucrose (\circ), 1 M trehalose (\triangle), 1 M D-glucose (∇), 1 M betaine (\diamond) and 1 M Ect-OH (\triangleleft) in a medium containing 50 mM Mes-NaOH (pH 6.5), 35 mM NaCl, 50 mM CaCl_2 , 300 μM MnCl_2 and 50 μM DCPIP at a chlorophyll concentration of 200 $\mu\text{g}/\text{mL}$. The light intensity ($\lambda = 625 \text{ nm}$) during photoactivation was 35 $\mu\text{mol photon m}^{-2} \text{ s}^{-1}$. The measurements of the oxygen evolution rate in the samples were carried out in 50 mM Mes-NaOH (pH 6.5), 35 mM NaCl and 50 mM CaCl_2 in the presence of exogenous electron acceptors $-1 \text{ mM K}_3[\text{Fe}(\text{CN})_6]$ and 100 μM DCBQ at 20 $\mu\text{g Chl}/\text{mL}$ under continuous illumination of the samples ($\lambda > 650 \text{ nm}$, 1500 $\text{photon m}^{-2} \text{ s}^{-1}$). All experiments were repeated three times. Data are presented as mean values \pm standard deviation.

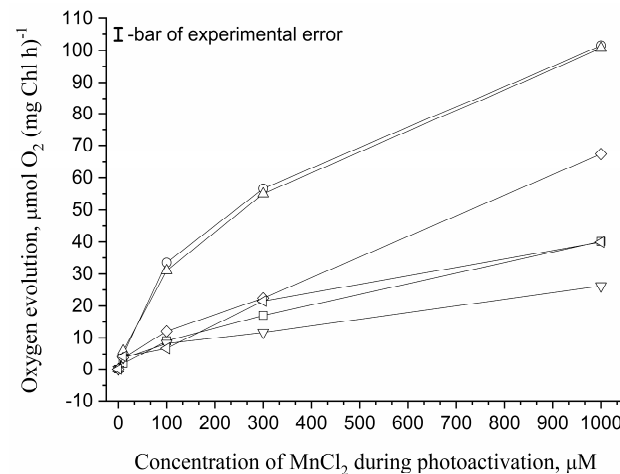


Figure 2. Dependence of the photoactivation of the O_2 -evolving activity in apo-WOC-PSII preparations on the concentration of MnCl_2 . Photoactivation was performed at different concentrations of MnCl_2 in the absence (\square) and in the presence of 1 M sucrose (\circ), 1 M trehalose (\triangle), 1 M D-glucose (∇), 1 M betaine (\diamond) and 1 M Ect-OH (\triangleleft) in a medium containing 50 mM Mes-NaOH (pH 6.5), 35 mM NaCl, 50 mM CaCl_2 and 50 μM DCPIP at a chlorophyll concentration of 200 $\mu\text{g}/\text{mL}$. The light intensity ($\lambda = 625 \text{ nm}$) during 30 min photoactivation was 35 $\mu\text{mol photon m}^{-2} \text{ s}^{-1}$. The measurement of the rate of oxygen evolution in the samples was carried out in a medium containing 50 mM Mes-NaOH (pH 6.5), 35 mM NaCl and 50 mM CaCl_2 in the presence of exogenous electron acceptors $-1 \text{ mM K}_3[\text{Fe}(\text{CN})_6]$ and 100 μM DCBQ at 20 $\mu\text{g Chl}/\text{mL}$ under continuous illumination

of the samples ($\lambda > 650$ nm, $1500 \mu\text{mol photon m}^{-2} \text{s}^{-1}$). All experiments were repeated three times. Data are presented as mean values \pm standard deviation.

The disaccharides enhance the efficiency of the photoassembly of a Mn_4CaO_5 cluster by 3.5 times if the photoactivation of apo-WOC-PSII was performed in the presence of 100–300 $\mu\text{M Mn}^{2+}$ and 2.5 times at 1 mM Mn^{2+} . The decreased stimulatory effect of disaccharides at 1 mM Mn^{2+} may be due to the fact that the ability of apo-WOC-PSII to photooxidize Mn^{2+} improves with increasing Mn^{2+} concentration. Betaine and Ect-OH slightly stimulated the photoactivation of apo-WOC-PSII, except betaine stimulated the photoactivation by 70% at 1 mM added Mn^{2+} . D-glucose did not stimulate the photoassembly of the Mn_4CaO_5 cluster but suppressed the photoactivation of apo-WOC-PSII preparations.

The first event of the photoassembly of the Mn_4CaO_5 cluster is the photooxidation of Mn^{2+} to Mn^{3+} at the high affinity manganese binding site. This process requires charge separation in the PSII reaction center with the formation of strong oxidants $\text{P}_{680}^{+\bullet}$ and TyrZ^\bullet . However, the formation of the oxidants can also lead to damage to PSII by the donor mechanism. In addition, it is necessary to stabilize the intermediate formed during the photoassembly of the inorganic core of the WOC as well as the newly assembled Mn_4CaO_5 cluster. It seems that the efficiency of the photoassembly of the Mn_4CaO_5 cluster in apo-WOC-PSII depends on the following factors: (1) the ability of RC PSII to oxidize Mn^{2+} ; (2) the prevention of the formation of long-lived forms of $\text{P}_{680}^{+\bullet}$ and TyrZ^\bullet ; and (3) the stabilization of both intermediate products and the newly formed functionally active Mn_4CaO_5 cluster. Therefore, we studied the effect of osmolytes on Mn^{2+} photooxidation in apo-WOC-PSII, the photoinhibition of the samples, and the stability of CaCl_2 -PSII preparations as an analogue of the apo-WOC-PSII with the reassembled functionally active Mn_4CaO_5 cluster and heat-induced inhibition of electron transfer in PSII.

3.2. Effect of Osmolytes on Mn^{2+} Photooxidation in apo-WOC-PSII Preparations

Figure 3 demonstrates the dependence of the reactivation of Fv (as a ratio in the Fv/Fm) on the concentration of added Mn^{2+} in the absence and in the presence of osmolytes.

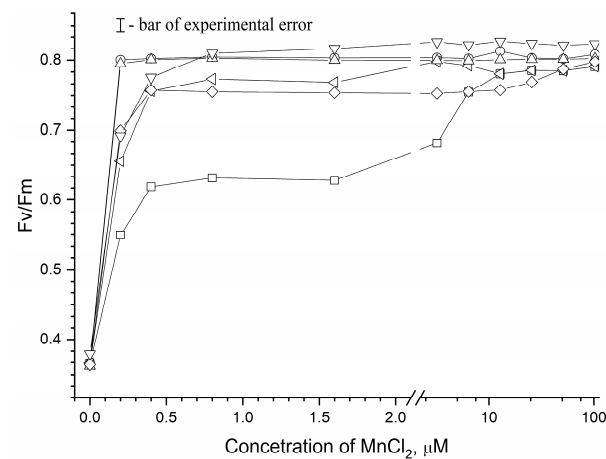


Figure 3. Dependence of the reactivation of photoinduced changes in the chlorophyll *a* fluorescence yield (Fv) on concentration of exogenous MnCl_2 . Fv reactivation was performed in the medium containing 50 mM Mes (pH 6.5), 35 mM NaCl in the absence of osmolyte (\square) and in the presence of 1 M sucrose (\circ), 1 M trehalose (\triangle), 1 M D-glucose (∇), 1 M betaine (\diamond) and 1 M Ect-OH (\triangleleft) at chlorophyll concentration of 10 $\mu\text{g}/\text{mL}$. All experiments were repeated three times. Data are presented as mean values \pm standard deviation.

As can be seen from this figure, the degree of reactivation of Fv increased with an increase in the concentration of Mn^{2+} . However, the ability of exogenous Mn^{2+} to reactivate Fv strongly depended on the presence of osmolytes. The maximum reactivation of Fv was reached at 0.2 $\mu\text{M Mn}^{2+}$ in the presence of 1 M sucrose or 1 M trehalose, about 0.4 μM

Mn^{2+} in the presence of 1 M D-glucose, 1 M Ect-OH or 1 M betaine, and 12 $\mu M Mn^{2+}$ in the absence of osmolyte. The results show that trehalose and sucrose more effectively stimulate Mn^{2+} photooxidation via the apo-WOC-PSII reaction centers.

3.3. Effect of Osmolytes on Mn-Induced Protection of apo-WOC-PSII against Photoinhibition

Figure 4 shows the effect of osmolytes on the photoinhibition of apo-WOC-PSII preparations dependent on the concentration of added Mn^{2+} . The degree of photoinhibition of apo-WOC-PSII preparations was determined based on the loss of the capability of PSII to be reactivated by sodium ascorbate.

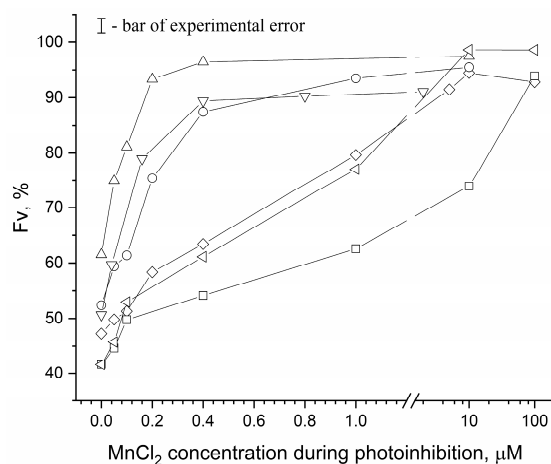


Figure 4. Dependence of photoinduced Fv measured in the presence of 2 mM sodium ascorbate in apo-WOC-PSII preparations which were exposed to inhibitory light ($\lambda = 625 \text{ nm}$, $15 \mu\text{mol photon m}^{-2} \text{ s}^{-1}$) for 5 min in the presence of various concentration of $MnCl_2$. Photoinhibition was performed in the medium containing 50 mM Mes (pH 6.5) and 35 mM NaCl at 20 $\mu\text{g Chl/mL}$ in the absence (\square) and in the presence of 1 M sucrose (\circ), 1 M trehalose (\triangle), 1 M D-glucose (∇), 1 M betaine (\diamond), and 1 M Ect-OH (\triangleleft). The measurement of Fv was carried out in the medium containing 50 mM Mes (pH 6.5), 35 mM NaCl and 2 mM sodium ascorbate at 10 $\mu\text{g Chl/mL}$. The amplitude Fv measured in apo-WOC-PSII preparations in the presence of 2 mM sodium ascorbate before photoinhibition was taken as 100%. All experiments were repeated three times. Data are presented as mean values \pm standard deviation.

As shown in Figure 4, the 5 min exposition of apo-WOC-PSII preparations to light with an intensity of $15 \mu\text{mol photon m}^{-2} \text{ s}^{-1}$ in the absence of added Mn^{2+} led to 60% photoinhibition. This is consistent with previous results showing the high sensitivity of apo-WOC-PSII to photoinhibition [31,85]. The addition of Mn^{2+} led to a decrease in the degree of photoinhibition of apo-WOC-PSII. The presence of osmolytes significantly enhanced the protective effect of Mn^{2+} against photoinhibition. In the absence of osmolytes, 50% protection of apo-WOC-PSII was observed at 10 $\mu M Mn^{2+}$, as well as in the presence of 1 M betaine and Ect-OH at 1 $\mu M Mn^{2+}$, 1 M D-glucose at 0.16 $\mu M Mn^{2+}$, 1 M sucrose at 0.2 $\mu M Mn^{2+}$ and 1 M trehalose at 0.1 $\mu M Mn^{2+}$.

3.4. Osmolyte Effect on Stability of Mn_4CaO_5 Cluster in $CaCl_2$ -PSII Preparations

To elucidate whether the effect of osmolytes on the photoactivation of apo-WOC-PSII is related to the stabilization of the newly assembled Mn_4CaO_5 cluster, we studied the effect of osmolytes on the stability of $CaCl_2$ -PSII preparations (Figure 5). The incubation of $CaCl_2$ -PSII preparations at 25 °C (the temperature at which photoactivation was performed) resulted in the suppression of oxygen-evolving activity in the samples, which before the incubation, was $56 \mu\text{mol O}_2 (\text{mg Chl h})^{-1}$. In the absence of osmolytes, the samples lost about 50% of their oxygen-evolving activity after 15 min of incubation. The presence of osmolytes decreased the loss of oxygen-evolving activity in the samples. However, osmolytes differed in the protective efficiency. In the presence of Ect-OH, a 50% decrease in oxygen-evolving activity was observed after 20 min of incubation, while in the presence of

D-glucose and betaine, the samples lost about 45% of their oxygen-evolving activity only after 30 min of incubation. Trehalose and sucrose showed the greatest protective effect: the oxygen-evolving activity of the samples after the 30 min incubation was reduced by only 30%.

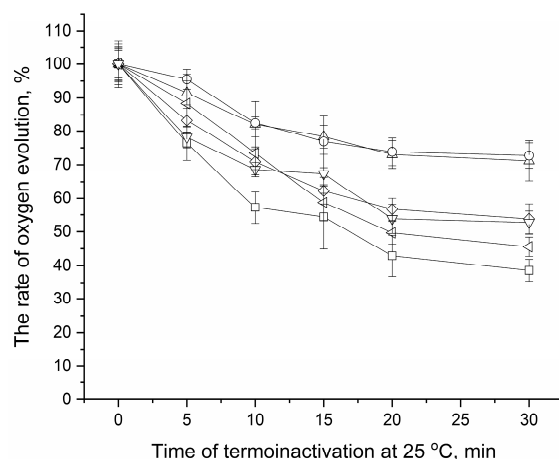


Figure 5. Dependence of O_2 -evolving activity in $CaCl_2$ -PSII preparations on time of incubation of preparation at 25 °C. The incubation was performed in the dark at 110 μg Chl/mL in the medium containing 50 mM Mes (pH 6.5), 35 mM NaCl and 20 mM Ca^{2+} (medium A) in the absence (\square) or in the presence of 1 M sucrose (\circ), 1 M trehalose (\triangle), 1 M D-glucose (∇), 1 M betaine (\diamond) and 1 M Ect-OH (\triangleleft). Light-induced oxygen evolution in the $CaCl_2$ -PSII preparations was measured in medium A in the presence of the electron acceptors (1 mM ferricyanide and 100 μM DCBQ) after 11 times dilutions of the samples. The rate of oxygen evolution in $CaCl_2$ -treated PSII preparations before the incubation (56 $\mu mol O_2$ (mg Chl h) $^{-1}$) was taken as 100%. All experiments were repeated three times. Data are presented as mean values \pm standard deviation.

3.5. Effect of Osmolytes on Heat-Induced Inhibition of Electron Transfer in PSII

Using PSII particles with intact WOC, we employed an analysis of a fast (within one second) polyphasic rise in chlorophyll *a* fluorescence registered with a high time resolution to evaluate the degree of heat-induced inhibition of electron transfer in PSII. The double normalization of ChlF transients between 20 μs and 3 ms ($W_{OJ} = (F_t - F_0)/(F_j - F_0)$) and between 20 μs and 30 ms ($W_{OI} = (F_t - F_0)/(F_I - F_0)$) in combination with the generation of difference kinetics (ΔW_{OJ} and ΔW_{OI} ; “after heat treatment” – “before heat treatment”) allowed for the visualization of so-called K-bands and J-bands, respectively. The K-band is believed to be associated with the disturbance of the water oxidation complex, and the J-band arises from the inhibition of electron transfer from Q_A to Q_B [86–88]. In the absence of osmolytes, an appearance of positive K-bands in ΔW_{OJ} and J-bands in ΔW_{OI} is observed after the incubation of PSII preparations for 40 min at 30 °C (Figure 6). The amplitude of the K-band became 75% lower when the incubation of the samples was performed in the presence of the osmolytes. The osmolytes also decreased the J-band, but in contrast to the K-band, their effects were different: the presence of trehalose or sucrose reduced the J-band by 50–55%, that of betaine reduced the J-band by 30% and that of Ect-OH reduced the J-band by 10%.

Fixed-length ultrasonic interferometry was used to determine the kinetics of damage to PSII preparations with an intact WOC during their incubation at 25 °C. Figure 7A demonstrates that the incubation of a suspension containing the PSII preparations at 25 °C led to a gradual decrease in the relative velocity of the ultrasound, probably due to the aggregation of PSII complexes. Refractometric measurements confirmed the aggregation of the preparations [89], which was more intense in the absence of osmolytes (Figure 8). After 40–45 min of incubation, a sharp increase in the ultrasound velocity was observed, which reflects the dissociation of the proteins of the water-oxidizing complex [84]. The absence of such an increase in ultrasound velocity during the incubation of $NaCl$ -PSII and $CaCl_2$ -PSII

preparations (Figure 9) may indicate that in native preparations, incubation leads to the dissociation of PsbP and PsbQ proteins from the WOC. The addition of osmolytes delayed the onset of the increase in ultrasound velocity (Figure 7B–F), which may reflect an increase in the WOC stability.

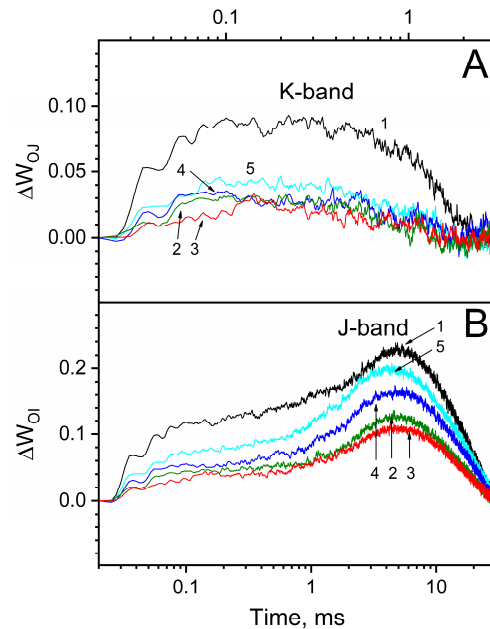


Figure 6. Difference kinetics ΔW_{OJ} and ΔW_{OI} showing K-band (A) and J-band (B) formation in ChlF transients double-normalized between F_0 and F_J phases, $W_{OJ} = (F_t - F_0)/(F_J - F_0)$, and between F_0 and F_I phases, $W_{OI} = (F_t - F_0)/(F_I - F_0)$, induced by heat treatment of PSII membrane fragments. Heat treatment (HT, 30 °C, 40 min) was performed in darkness in the absence of osmolytes (1) and in the presence of 1 M sucrose (2), 1 M trehalose (3), 1 M betaine (4) and 1 M Ect-OH (5) in a medium containing 50 mM Mes (pH 6.5) and 35 mM NaCl at 10 μg Chl/mL. The presented kinetics are the differences $\Delta W_{OJ} = [W_{OJ} \text{ after HT} - W_{OJ} \text{ before HT}]$ and $\Delta W_{OI} = [W_{OI} \text{ after HT} - W_{OI} \text{ before HT}]$ of the average for 4 “before HT” and 5 “after HT” independent curves. In all experiments, Fv was induced by a single 880 ms saturating flash ($\lambda = 625 \text{ nm}$, $2360 \mu\text{mol photons m}^{-2} \text{ s}^{-1}$). Measurements were performed in a medium containing 50 mM Mes (pH 6.5) and 35 mM NaCl at 10 μg Chl/mL at room temperature, 25 °C.

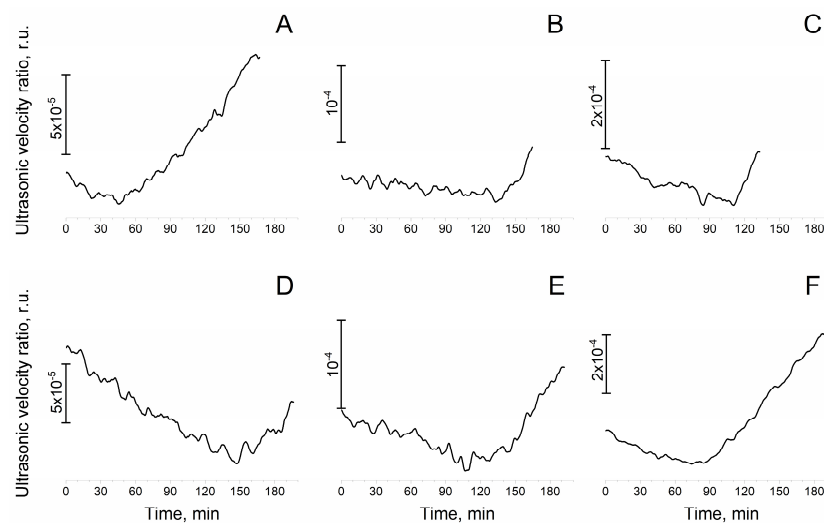


Figure 7. Changes in the relative velocity of ultrasound in the suspension containing photosystem II preparations with the native water-oxidizing complex during their incubation at 25 °C. Measurements

were performed in the medium containing 50 mM Mes (pH 6.5) and 35 mM NaCl in the absence (A) and in the presence of 1 M sucrose (B), 1 M trehalose (C), 1 M D-glucose (D), 1 M betaine (E) and 1 M Ect-OH (F) at 200 μg Chl/mL and were repeated at least three times.

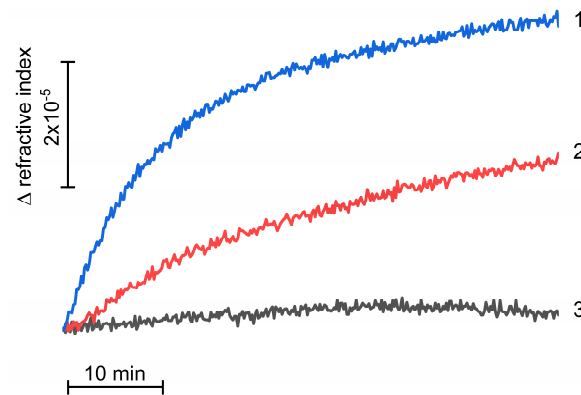


Figure 8. Changes in the refractive index in the suspension containing photosystem II preparations with the native water-oxidizing complex in the absence (1) and in the presence of 1 M trehalose (2) during their incubation at 25 °C. Curve 3 reflects changes in the refractive index in 1 M trehalose solution without PSII preparations. Measurements were performed in the medium containing 50 mM Mes (pH 6.5) and 35 mM NaCl at 200 μg Chl/mL and were repeated at least three times.

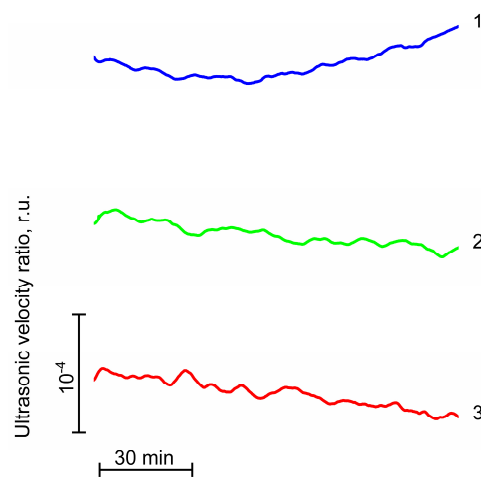


Figure 9. Changes in the relative velocity of ultrasound in the suspension containing photosystem II preparations with the native water-oxidizing complex (1), NaCl-PSII preparations (2) and CaCl_2 -PSII preparations (3) during their incubation at 25 °C. Measurements were performed in the medium containing 50 mM Mes (pH 6.5) and 35 mM NaCl at 200 μg Chl/mL and were repeated at least three times.

4. Discussion

One of the most sensitive sites of the photosynthetic electron transport chain of plants to various stress factors is photosystem II [10], which is capable of photogenerating the strongest biological oxidant [1–3] and contains a relatively unstable water-oxidizing complex. As a result, plants are forced to constantly restore damaged PSII complexes through the activation of the photoassembly process, which includes the process of photoformation of the water-oxidizing complex. This is most pronounced when plants grow under conditions of high solar insolation, elevated temperatures and lack of water. The synthesis and accumulation of osmolytes is one of the main strategies used by plants in response to various stress factors [90–97]. Our results for the first time show that the presence of trehalose and sucrose during photoactivation of the apo-WOC-PSII significantly increases the efficiency of the photoassembly of a Mn_4CaO_5 cluster. Samples photoactivated in the

presence of these osmolytes showed much higher rates of light-induced oxygen evolution than samples photoactivated in the absence of osmolytes (Figures 1 and 2). Other osmolytes either slightly stimulated the photoassembly of the Mn_4CaO_5 cluster (betaine and Ect-OH) or had a negative effect (D-glucose). This is probably due to their effect on factors influencing the photoassembly of the Mn_4CaO_5 cluster. The effectiveness of osmolytes will depend on their ability (i) to improve the photooxidation of Mn^{2+} by PSII RC; (ii) to reduce the photoinhibition of PSII; (iii) to stabilize the WOC and the electron transport; and (iv) to be inert towards the intermediates formed during the photoactivation.

Firstly, Mn^{2+} photooxidation improved due to the reaction centers of apo-WOC-PSII. The reactivation of Fv in apo-WOC-PSII by added Mn^{2+} (which may indicate the ability of apo-WOC-PSII to photooxidize Mn^{2+}) significantly increases in the presence of osmolytes. Maximum Fv restoration required 60 times less concentration of added Mn^{2+} in the presence of trehalose or sucrose and about 30 times less in the presence of betaine, Ect-OH or D-glucose (Figure 3). Thus, osmolytes, especially trehalose and sucrose, significantly stimulate electron donation from exogenous Mn^{2+} to the apo-WOC-PSII reaction center. This may indicate that structural changes in apo-WOC-PSII induced by osmolytes are important for the redox interaction of Mn^{2+} with the donor-side PSII. When studying the effect of sucrose on PSII, it was suggested that sucrose leads to structural alterations at the active site of the WOC via changes in the hydration of the protein complex and induces shifts in the pKa at the aspartic or glutamic acid side [65]. It is likely that these osmolyte-induced changes increase the binding of Mn^{2+} to apo-WOC-PSII and the ability of PSII reaction centers to photooxidize Mn^{2+} .

Secondly, the photoactivation of apo-WOC-PSII will depend on the protection of PSII from damage related to the donor side, since these preparations are very sensitive to photoinhibition induced by the formation of long-lived forms of $\text{P}_{680}^{+\bullet}$ or TyrZ^\bullet [31] and so the addition of Mn^{2+} suppresses photoinhibition. In the absence of osmolytes, the maximum protection of apo-WOC-PSII against photoinhibition was observed at 100 μM MnCl_2 (Figure 4). Osmolytes enhanced the protective effect of the added Mn^{2+} , although with varying efficiency. The maximum protection of apo-WOC-PSII against photoinhibition required 500 times less Mn^{2+} in the presence of trehalose and 250 times less Mn^{2+} in the presence of sucrose or D-glucose compared to that required in the absence of osmolytes. Betaine and Ect-OH showed the weakest effect on the Mn-dependent protection of apo-WOC-PSII against photoinhibition among the osmolytes: in the presence of betaine and Ect-OH, only 20 and 10 times less Mn^{2+} was required, respectively, to achieve the maximum protective effect. The results demonstrate that the protective effect of trehalose and sucrose against the photoinhibition of apo-WOC-PSII is manifested at lower concentrations of exogenous Mn^{2+} than the effect of betaine and Ect-OH that correlates with the effect of osmolytes on the reactivation of Fv in apo-WOC-PSII by added Mn^{2+} . This also may explain why betaine remarkably stimulated the photoactivation of apo-WOC-PSII only at high concentrations of added Mn^{2+} . Some osmolytes (especially trehalose) also showed a protective effect against the photoinhibition of apo-WOC-PSII preparations without added Mn^{2+} (Figure 4) that is in agreement with previous data [64]. This is probably due to the fact that apo-WOC-PSII can contain trace amounts of manganese. The influence of osmolytes on the effects of manganese described in Sections 3.2 and 3.3. has been partially investigated previously [64,68,75], and similar results were obtained. The use of apo-WOC-PSII preparations obtained by a different method (hydroxylamine treatment) in this study, which is slightly different from those used previously [15], makes it necessary to repeat these experiments.

Thirdly, it is known that osmolytes protect the water-oxidizing complex of PSII from termoinactivation [61,63]. This property of osmolytes can be responsible for the increase in the yield of photoactivation of apo-WOC-PSII due to the long photoactivation procedure (30 min, 25 °C) possibly being accompanied by the destruction of the photoassembled Mn_4CaO_5 cluster. By using CaCl_2 -PSII preparations (as an analogue of the apo-WOC-PSII with the photoassembled Mn_4CaO_5 cluster), it was revealed that the presence of

trehalose and sucrose significantly slowed down the loss in the oxygen-evolving activity of CaCl_2 -PSII during their incubation at 25 °C (Figure 5). The effect of other osmolytes was not as striking as those of trehalose and sucrose. Thus, a significant enhancement in the efficiency of the photoactivation of apo-WOC-PSII by trehalose and sucrose can be associated with changes in apo-WOC-PSII that are important for manganese cluster photoassembly: improvement in the photooxidation of Mn^{2+} to Mn^{3+} by reaction centers of PSII, protection of PSII from damage induced by the formation of long-lived forms of $\text{P}_{680}^{+\bullet}$ or TyrZ^\bullet , and stabilization of either a metastable intermediate complex or the formed functionally active Mn_4CaO_5 cluster. In addition, osmolytes stabilize the water-oxidizing complex, preventing the dissociation of the extrinsic proteins of the complex (Figure 7). This property of osmolytes may be manifested in the function and photoassembly of the WOC during the photorecovery of PSII in vivo. In our experiments (Figure 8) and early works [47,71], it was shown that osmolytes can prevent the aggregation of PSII preparations during long-term storage. This property of osmolytes may in turn improve the efficiency of Mn cluster photoassembly.

Weak stimulation of the photoactivation of apo-WOC-PSII by betaine and Ect-OH correlates with their effects on the above-listed factors. However, D-glucose, which improved the restoration of Fv by Mn^{2+} , enhanced the protective effect of added Mn^{2+} against the photoinhibition of apo-WOC-PSII and increased the stability of CaCl_2 -PSII preparations, at the same time decreasing the efficiency of the photoassembly of the Mn_4CaO_5 cluster. It was shown that Mn(III) is capable of oxidizing D-glucose [98]. Therefore, the negative effect of D-glucose on the photoactivation of apo-WOC-PSII may be due to its redox interaction with Mn(III), formed as a result of the oxidation of Mn^{2+} by the RC of apo-WOC-PSII. This interaction may eliminate the formation of metastable products necessary for the formation of a Mn_4CaO_5 cluster.

The effective electron transfer within reaction centers of apo-WOC-PSII is necessary for the photoassembly of a Mn_4CaO_5 cluster, so blocking of the electron transfer from Q_A to Q_B may reduce the yield of photoactivation of the apo-WOC-PSII. The incubation of PSII preparations with an intact WOC for 40 min at 30 °C led to the appearance of J-bands, which were detected after subtracting the double-normalized kinetics obtained after and before incubation of the samples at 30 °C (Figure 6B). A J-band is believed to appear as a result of the inhibition of electron transfer from Q_A to Q_B [86–88]. Trehalose and sucrose, in comparison with other osmolytes (betaine and Ect-OH), significantly reduced the amplitude of J-bands (Figure 6B). Recently, it was shown that the addition of trehalose led to a significant increase in the rate of electron transfer between Q_A and Q_B as well as to the almost complete disappearance of “closed RCs of PSII”, where the electron transfer between Q_A and Q_B was blocked [75]. It seems that sucrose (like trehalose) may also stabilize electron transport from Q_A to Q_B in apo-WOC-PSII preparations during the photoactivation procedure. The stabilization of electron transport in $\text{Q}_A - \text{Q}_B$ sites may also be important for the increase in the yield of photoactivation of apo-WOC-PSII.

Thus, the stimulation of the photoassembly of Mn_4CaO_5 clusters in apo-WOC-PSII by osmolytes will appear if, on the one hand, the osmolytes improve the photooxidation of Mn^{2+} by RC, reduce the photoinhibition of PSII and stabilize the WOC after the photoassembly of a functionally active Mn_4CaO_5 cluster as well as electron transport from Q_A to Q_B and, on the other hand, they do not interact with intermediate products formed during the photooxidation of bound Mn^{2+} in apo-WOC-PSII. The different influences of osmolytes on the photoassembly of a Mn_4CaO_5 cluster apparently depends on their effect on the protein structures of PSII in terms of the interactions with water molecules.

It is suggested that trehalose may change protein packing to the more optimal conformation and/or cause protein–protein interactions in the WOC, which increase the rate of turnover of S-state transitions and, consequently, the efficiency of water photooxidation and oxygen evolution [99]. It seems that such changes induced by trehalose also may promote the efficiency of Mn_4CaO_5 cluster photoassembly. So, the significant effect of trehalose and sucrose may be due to the fact that trehalose and sucrose are classified as osmolytes,

which stabilize proteins that increase the free energy of both native and denatured states, and therefore, their role in PSII photoactivation can be compared to chaperones [100]. Betaine, which also stimulated the photoactivation of apo-WOC-PSII at high Mn^{2+} concentrations (but almost two times less than sucrose and trehalose), is attributed to the moderate alteration of osmolyte proteins [100].

The stimulating effect of osmolytes (especially of disaccharides) on the photoactivation of apo-WOC-PSII revealed in the present study may occur in vivo during the photo-driven formation and reparation of PSII. These processes include the WOC photoformation step, during which photosystem II is most susceptible to photodamage. The concentration of disaccharides in plant chloroplasts is strongly dependent on the plant species. For example, the amount of sucrose in chloroplasts can reach 15–30% of the amount of sucrose in pro-toplasts [101–104]. Chloroplasts are able to import sugars (including sucrose) across their membranes using specific transport proteins [104–107]. For example, plastidic sugar transporter (pSuT) has been reported to transport sucrose across the chloroplast membrane [108]. It has also been proposed that the chloroplast might act as a sucrose reservoir [108].

Author Contributions: Conceptualization, methodology A.A.K. and D.V.Y.; investigation A.A.K., D.V.K. and D.V.Y.; writing—original draft preparation A.A.K.; funding acquisition D.V.K. All authors have read and agreed to the published version of the manuscript.

Funding: The work was supported by the Russian Science Foundation Grant No. 22-24-01179, <https://rscf.ru/project/22-24-01179/> (accessed on 19 September 2023).

Data Availability Statement: Data are contained within the article.

Acknowledgments: PAM fluorometry was carried out using the MULTI-COLOR PAM fluorometer of the Pushchino Center of Biological Research RAS (<https://ckp-rf.ru/ckp/670266/> (accessed on 12 December 2023)).

Conflicts of Interest: The authors declare no conflict of interest.

References

1. Klimov, V.; Allakhverdiev, S.; Demeter, S.; Krasnovsky, A. Photoreduction of pheophytin in chloroplast photosystem II as a function of the redox potential of the medium. *Dokl. Akad. Nauk SSSR* **1979**, *249*, 227–230.
2. Ishikita, H.; Loll, B.; Biesiadka, J.; Saenger, W.; Knapp, E.-W. Redox potentials of chlorophylls in the photosystem II reaction center. *Biochemistry* **2005**, *44*, 4118–4124. [[CrossRef](#)] [[PubMed](#)]
3. Allakhverdiev, S.I.; Tomo, T.; Shimada, Y.; Kindo, H.; Nagao, R.; Klimov, V.V.; Mimuro, M. Redox potential of pheophytin a in photosystem II of two cyanobacteria having the different special pair chlorophylls. *Proc. Natl. Acad. Sci. USA* **2010**, *107*, 3924–3929. [[CrossRef](#)] [[PubMed](#)]
4. Ludlow, M.M. *Light Stress at High Temperature*; Elsevier: New York, NY, USA, 1987.
5. Masojidek, J.; Trivedi, S.; Halshaw, L.; Alexiou, A.; Hall, D.O. The synergistic effect of drought and light stresses in sorghum and pearl millet. *Plant Physiol.* **1991**, *96*, 198–207. [[CrossRef](#)] [[PubMed](#)]
6. Ögren, E. The significance of photoinhibition for photosynthetic productivity. In *Photoinhibition of Photosynthesis from Molecular Mechanisms to the Field*; Bios Scientific Publishers: Oxford, UK, 1994; pp. 433–447.
7. Goh, C.-H.; Ko, S.-M.; Koh, S.; Kim, Y.-J.; Bae, H.-J. Photosynthesis and environments: Photoinhibition and repair mechanisms in plants. *J. Plant Biol.* **2012**, *55*, 93–101. [[CrossRef](#)]
8. Long, S.P.; Humphries, S.; Falkowski, P.G. Photoinhibition of photosynthesis in nature. *Annu. Rev. Plant Biol.* **1994**, *45*, 633–662. [[CrossRef](#)]
9. Tikkanen, M.; Grieco, M.; Nurmi, M.; Rantala, M.; Suorsa, M.; Aro, E.-M. Regulation of the photosynthetic apparatus under fluctuating growth light. *Philos. Trans. R. Soc. B Biol. Sci.* **2012**, *367*, 3486–3493. [[CrossRef](#)]
10. Powles, S.B. Photoinhibition of photosynthesis induced by visible light. *Annu. Rev. Plant Physiol.* **1984**, *35*, 15–44. [[CrossRef](#)]
11. Aro, E.-M.; Virgin, I.; Andersson, B. Photoinhibition of photosystem II. Inactivation, protein damage and turnover. *Biochim. Biophys. Acta (BBA)—Bioenerg.* **1993**, *1143*, 113–134. [[CrossRef](#)]
12. Tyystjärvi, E. Photoinhibition of photosystem II. *Int. Rev. Cell Mol. Biol.* **2013**, *300*, 243–303.
13. Radmer, R.; Cheniae, G.M. Photoactivation of the manganese catalyst of O_2 evolution. II. A two-quantum mechanism. *Biochim. Biophys. Acta (BBA)—Bioenerg.* **1971**, *253*, 182–186. [[CrossRef](#)]
14. Tamura, N.; Cheniae, G. Requirements for the photoligation of Mn^{2+} in PS II membranes and the expression of water-oxidizing activity of the polynuclear Mn-catalyst. *FEBS Lett.* **1986**, *200*, 231–236. [[CrossRef](#)]

15. Tamura, N.; Cheniae, G. Photoactivation of the water-oxidizing complex in photosystem II membranes depleted of Mn and extrinsic proteins. I. Biochemical and kinetic characterization. *Biochim. Biophys. Acta (BBA)—Bioenerg.* **1987**, *890*, 179–194. [[CrossRef](#)]
16. Miller, A.F.; Brudvig, G.W. Manganese and calcium requirements for reconstitution of oxygen-evolution activity in manganese-depleted photosystem II membranes. *Biochemistry* **1989**, *28*, 8181–8190. [[CrossRef](#)] [[PubMed](#)]
17. Tamura, N.; Inoue, Y.; Cheniae, G.M. Photoactivation of the water-oxidizing complex in Photosystem II membranes depleted of Mn, Ca and extrinsic proteins: II. Studies on the functions of Ca^{2+} . *Biochim. Biophys. Acta (BBA)—Bioenerg.* **1989**, *976*, 173–181. [[CrossRef](#)]
18. Miyao, M.; Inoue, Y. An improved procedure for photoactivation of photosynthetic oxygen evolution: Effect of artificial electron acceptors on the photoactivation yield of NH_2OH -treated wheat photosystem II membranes. *Biochim. Biophys. Acta (BBA)—Bioenerg.* **1991**, *1056*, 47–56. [[CrossRef](#)]
19. Ananyev, G.M.; Dismukes, G.C. Assembly of the tetra-Mn site of photosynthetic water oxidation by photoactivation: Mn stoichiometry and detection of a new intermediate. *Biochemistry* **1996**, *35*, 4102–4109. [[CrossRef](#)]
20. Ananyev, G.M.; Dismukes, G.C. High-resolution kinetic studies of the reassembly of the tetra-manganese cluster of photosynthetic water oxidation: Proton equilibrium, cations, and electrostatics. *Biochemistry* **1996**, *35*, 14608–14617. [[CrossRef](#)]
21. Ananyev, G.M.; Dismukes, G.C. Calcium induces binding and formation of a spin-coupled dimanganese (II,II) center in the apo-water oxidation complex of photosystem II as precursor to the functional tetra-Mn/Ca cluster. *Biochemistry* **1997**, *36*, 11342–11350. [[CrossRef](#)]
22. Zaltsman, L.; Ananyev, G.M.; Bruntrager, E.; Dismukes, G.C. Quantitative kinetic model for photoassembly of the photosynthetic water oxidase from its inorganic constituents: Requirements for manganese and calcium in the kinetically resolved steps. *Biochemistry* **1997**, *36*, 8914–8922. [[CrossRef](#)]
23. Baranov, S.V.; Ananyev, G.M.; Klimov, V.V.; Dismukes, G.C. Bicarbonate accelerates assembly of the inorganic core of the water-oxidizing complex in manganese-depleted photosystem II: A proposed biogeochemical role for atmospheric carbon dioxide in oxygenic photosynthesis. *Biochemistry* **2000**, *39*, 6060–6065. [[CrossRef](#)] [[PubMed](#)]
24. Baranov, S.; Tyryshkin, A.; Katz, D.; Dismukes, G.; Ananyev, G.; Klimov, V. Bicarbonate is a native cofactor for assembly of the manganese cluster of the photosynthetic water oxidizing complex. Kinetics of reconstitution of O_2 evolution by photoactivation. *Biochemistry* **2004**, *43*, 2070–2079. [[CrossRef](#)] [[PubMed](#)]
25. Miyao-Tokutomi, M.; Inoue, Y. Improvement by benzoquinones of the quantum yield of photoactivation of photosynthetic oxygen evolution: Direct evidence for the two-quantum mechanism. *Biochemistry* **1992**, *31*, 526–532. [[CrossRef](#)] [[PubMed](#)]
26. Khorobrykh, A. A possible relationship between the effect of factors on photoactivation of photosystem II depleted of functional Mn and cytochrome b559. *Biochim. Biophys. Acta (BBA)—Bioenerg.* **2023**, *1864*, 148997. [[CrossRef](#)] [[PubMed](#)]
27. Khorobrykh, A.A.; Yanykin, D.V.; Klimov, V.V. Enhancement of photoassembly of the functionally active water-oxidizing complex in Mn-depleted photosystem II membranes upon transition to anaerobic conditions. *J. Photochem. Photobiol. B Biol.* **2016**, *163*, 211–215. [[CrossRef](#)] [[PubMed](#)]
28. Dasgupta, J.; Ananyev, G.M.; Dismukes, G.C. Photoassembly of the water-oxidizing complex in photosystem II. *Coord. Chem. Rev.* **2008**, *252*, 347–360. [[CrossRef](#)] [[PubMed](#)]
29. Bao, H.; Burnap, R.L. Photoactivation: The light-driven assembly of the water oxidation complex of photosystem II. *Front. Plant Sci.* **2016**, *7*, 578. [[CrossRef](#)] [[PubMed](#)]
30. Zhang, M.; Bommer, M.; Chatterjee, R.; Hussein, R.; Yano, J.; Dau, H.; Kern, J.; Dobbek, H.; Zouni, A. Structural insights into the light-driven auto-assembly process of the water-oxidizing Mn_4CaO_5 -cluster in photosystem II. *eLife* **2017**, *6*, e26933. [[CrossRef](#)]
31. Klimov, V.; Shafiev, M.; Allakhverdiev, S. Photoinactivation of the reactivation capacity of photosystem II in pea subchloroplast particles after a complete removal of manganese. *Photosynth. Res.* **1990**, *23*, 59–65. [[CrossRef](#)]
32. Jegerschoeld, C.; Virgin, I.; Styring, S. Light-dependent degradation of the D1 protein in photosystem II is accelerated after inhibition of the water splitting reaction. *Biochemistry* **1990**, *29*, 6179–6186. [[CrossRef](#)]
33. Telfer, A.; De Las Rivas, J.; Barber, J. β -Carotene within the isolated Photosystem II reaction centre: Photooxidation and irreversible bleaching of this chromophore by oxidised P680. *Biochim. Biophys. Acta (BBA)—Bioenerg.* **1991**, *1060*, 106–114. [[CrossRef](#)]
34. Wang, W.-Q.; Chapman, D.J.; Barber, J. Inhibition of water splitting increases the susceptibility of photosystem II to photoinhibition. *Plant Physiol.* **1992**, *99*, 16–20. [[CrossRef](#)] [[PubMed](#)]
35. Kurepin, L.V.; Ivanov, A.G.; Zaman, M.; Pharis, R.P.; Allakhverdiev, S.I.; Hurry, V.; Hüner, N.P. Stress-related hormones and glycinebetaine interplay in protection of photosynthesis under abiotic stress conditions. *Photosynth. Res.* **2015**, *126*, 221–235. [[CrossRef](#)] [[PubMed](#)]
36. Khan, M.S.; Yu, X.; Kikuchi, A.; Asahina, M.; Watanabe, K.N. Genetic engineering of glycine betaine biosynthesis to enhance abiotic stress tolerance in plants. *Plant Biotechnol.* **2009**, *26*, 125–134. [[CrossRef](#)]
37. Jewell, M.C.; Campbell, B.C.; Godwin, I.D. Transgenic plants for abiotic stress resistance. In *Transgenic Crop Plants*; Springer: Berlin/Heidelberg, Germany, 2010; pp. 67–132.
38. Kumar, V.; Khare, T. Individual and additive effects of Na^+ and Cl^- ions on rice under salinity stress. *Arch. Agron. Soil Sci.* **2015**, *61*, 381–395. [[CrossRef](#)]
39. Ashraf, M.; Foolad, M.R. Roles of glycine betaine and proline in improving plant abiotic stress resistance. *Environ. Exp. Bot.* **2007**, *59*, 206–216. [[CrossRef](#)]
40. Sicher, R.C.; Timlin, D.; Bailey, B. Responses of growth and primary metabolism of water-stressed barley roots to rehydration. *J. Plant Physiol.* **2012**, *169*, 686–695. [[CrossRef](#)] [[PubMed](#)]

41. Keunen, E.; Peshev, D.; Vangronsveld, J.; Van Den Ende, W.; Cuyper, A. Plant sugars are crucial players in the oxidative challenge during abiotic stress: Extending the traditional concept. *Plant Cell Environ.* **2013**, *36*, 1242–1255. [[CrossRef](#)]
42. Whittaker, A.; Bochicchio, A.; Vazzana, C.; Lindsey, G.; Farrant, J. Changes in leaf hexokinase activity and metabolite levels in response to drying in the desiccation-tolerant species *Sporobolus stapfianus* and *Xerophyta viscosa*. *J. Exp. Bot.* **2001**, *52*, 961–969. [[CrossRef](#)]
43. Moore, J.P.; Hearshaw, M.; Ravenscroft, N.; Lindsey, G.G.; Farrant, J.M.; Brandt, W.F. Desiccation-induced ultrastructural and biochemical changes in the leaves of the resurrection plant *Myrothamnus flabellifolia*. *Aust. J. Bot.* **2007**, *55*, 482–491. [[CrossRef](#)]
44. Peters, S.; Mundree, S.G.; Thomson, J.A.; Farrant, J.M.; Keller, F. Protection mechanisms in the resurrection plant *Xerophyta viscosa* (Baker): Both sucrose and raffinose family oligosaccharides (RFOs) accumulate in leaves in response to water deficit. *J. Exp. Bot.* **2007**, *58*, 1947–1956. [[CrossRef](#)] [[PubMed](#)]
45. Hoekstra, F.A.; Golovina, E.A.; Buitink, J. Mechanisms of plant desiccation tolerance. *Trends Plant Sci.* **2001**, *6*, 431–438. [[CrossRef](#)] [[PubMed](#)]
46. Martinelli, T. In situ localization of glucose and sucrose in dehydrating leaves of *Sporobolus stapfianus*. *J. Plant Physiol.* **2008**, *165*, 580–587. [[CrossRef](#)] [[PubMed](#)]
47. Goyal, K.; Walton, L.J.; Tunnacliffe, A. LEA proteins prevent protein aggregation due to water stress. *Biochem. J.* **2005**, *388*, 151–157. [[CrossRef](#)] [[PubMed](#)]
48. Crowe, L.M. Lessons from nature: The role of sugars in anhydrobiosis. *Comp. Biochem. Physiol. Part A Mol. Integr. Physiol.* **2002**, *131*, 505–513. [[CrossRef](#)] [[PubMed](#)]
49. Francia, F.; Malferrari, M.; Sacquin-Mora, S.; Venturoli, G. Charge recombination kinetics and protein dynamics in wild type and carotenoid-less bacterial reaction centers: Studies in trehalose glasses. *J. Phys. Chem. B* **2009**, *113*, 10389–10398. [[CrossRef](#)] [[PubMed](#)]
50. Fernandez, O.; Béthencourt, L.; Quero, A.; Sangwan, R.S.; Clément, C. Trehalose and plant stress responses: Friend or foe? *Trends Plant Sci.* **2010**, *15*, 409–417. [[CrossRef](#)] [[PubMed](#)]
51. Lunn, J.E.; Delorge, I.; Figueroa, C.M.; Van Dijck, P.; Stitt, M. Trehalose metabolism in plants. *Plant J.* **2014**, *79*, 544–567. [[CrossRef](#)]
52. Crowe, J.H.; Hoekstra, F.A.; Crowe, L.M. Anhydrobiosis. *Annu. Rev. Physiol.* **1992**, *54*, 579–599. [[CrossRef](#)]
53. Jun, S.-S.; Choi, H.J.; Lee, H.Y.; Hong, Y.-N. Differential protection of photosynthetic capacity in trehalose-and LEA protein-producing transgenic plants under abiotic stresses. *J. Plant Biol.* **2008**, *51*, 327–336. [[CrossRef](#)]
54. Williams, B.; Njaci, I.; Moghaddam, L.; Long, H.; Dickman, M.B.; Zhang, X.; Mundree, S. Trehalose accumulation triggers autophagy during plant desiccation. *PLoS Genet.* **2015**, *11*, e1005705. [[CrossRef](#)] [[PubMed](#)]
55. Mostofa, M.G.; Hossain, M.A.; Fujita, M.; Tran, L.-S.P. Physiological and biochemical mechanisms associated with trehalose-induced copper-stress tolerance in rice. *Sci. Rep.* **2015**, *5*, 11433. [[CrossRef](#)] [[PubMed](#)]
56. Nunes, C.; Schluepmann, H.; Delatte, T.L.; Wingler, A.; Silva, A.B.; Fevereiro, P.S.; Jansen, M.; Fiorani, F.; Wiese-Klinkenberg, A.; Paul, M.J. Regulation of growth by the trehalose pathway: Relationship to temperature and sucrose. *Plant Signal. Behav.* **2013**, *8*, e26626. [[CrossRef](#)] [[PubMed](#)]
57. Zentella, R.; Mascorro-Gallardo, J.O.; Van Dijck, P.; Folch-Mallol, J.; Bonini, B.; Van Vaeck, C.; Gaxiola, R.; Covarrubias, A.A.; Nieto-Sotelo, J.; Thevelein, J.M. A *Selaginella lepidophylla* trehalose-6-phosphate synthase complements growth and stress-tolerance defects in a yeast *tps1* mutant. *Plant Physiol.* **1999**, *119*, 1473–1482. [[CrossRef](#)] [[PubMed](#)]
58. Papageorgiou, G.C.; Fujimura, Y.; Murata, N. Protection of the oxygen-evolving photosystem II complex by glycinebetaine. *Biochim. Biophys. Acta (BBA)—Bioenerg.* **1991**, *1057*, 361–366. [[CrossRef](#)]
59. Papageorgiou, G.C.; Murata, N. The unusually strong stabilizing effects of glycine betaine on the structure and function of the oxygen-evolving photosystem II complex. *Photosynth. Res.* **1995**, *44*, 243–252. [[CrossRef](#)] [[PubMed](#)]
60. Mohanty, P.; Hayashi, H.; Papageorgiou, G.; Murata, N. Stabilization of the Mn-cluster of the oxygen-evolving complex by glycinebetaine. *Biochim. Biophys. Acta (BBA)—Bioenerg.* **1993**, *1144*, 92–96. [[CrossRef](#)]
61. Allakhverdiev, S.; Feyziev, Y.M.; Ahmed, A.; Hayashi, H.; Aliev, J.A.; Klimov, V.; Murata, N.; Carpentier, R. Stabilization of oxygen evolution and primary electron transport reactions in photosystem II against heat stress with glycinebetaine and sucrose. *J. Photochem. Photobiol. B Biol.* **1996**, *34*, 149–157. [[CrossRef](#)]
62. Allakhverdiev, S.I.; Hayashi, H.; Nishiyama, Y.; Ivanov, A.G.; Aliev, J.A.; Klimov, V.V.; Murata, N.; Carpentier, R. Glycinebetaine protects the D1/D2/Cytb559 complex of photosystem II against photo-induced and heat-induced inactivation. *J. Plant Physiol.* **2003**, *160*, 41–49. [[CrossRef](#)]
63. Klimov, V.V.; Allakhverdiev, S.I.; Nishiyama, Y.; Khorobrykh, A.A.; Murata, N. Stabilization of the oxygen-evolving complex of photosystem II by bicarbonate and glycinebetaine in thylakoid and subthylakoid preparations. *Funct. Plant Biol.* **2003**, *30*, 797–803. [[CrossRef](#)]
64. Yanykin, D.; Khorobrykh, A.; Mamedov, M.; Klimov, V. Trehalose protects Mn-depleted photosystem 2 preparations against the donor-side photoinhibition. *J. Photochem. Photobiol. B Biol.* **2016**, *164*, 236–243. [[CrossRef](#)] [[PubMed](#)]
65. Halverson, K.M.; Barry, B.A. Sucrose and glycerol effects on photosystem II. *Biophys. J.* **2003**, *85*, 1317–1325. [[CrossRef](#)] [[PubMed](#)]
66. Mamedov, M.; Hayashi, H.; Wada, H.; Mohanty, P.; Papageorgiou, G.; Murata, N. Glycinebetaine enhances and stabilizes the evolution of oxygen and the synthesis of ATP by cyanobacterial thylakoid membranes. *FEBS Lett.* **1991**, *294*, 271–274. [[CrossRef](#)] [[PubMed](#)]
67. Murata, N.; Mohanty, P.; Hayashi, H.; Papageorgiou, G. Glycinebetaine stabilizes the association of extrinsic proteins with the photosynthetic oxygen-evolving complex. *FEBS Lett.* **1992**, *296*, 187–189. [[CrossRef](#)] [[PubMed](#)]

68. Yanykin, D.; Malferrari, M.; Rapino, S.; Venturoli, G.; Semenov, A.Y.; Mamedov, M. Hydroxyectoine protects Mn-depleted photosystem II against photoinhibition acting as a source of electrons. *Photosynth. Res.* **2019**, *141*, 165–179. [[CrossRef](#)] [[PubMed](#)]
69. Hinch, D.K. Low concentrations of trehalose protect isolated thylakoids against mechanical freeze-thaw damage. *Biochim. Biophys. Acta (BBA)—Biomembr.* **1989**, *987*, 231–234. [[CrossRef](#)]
70. Apostolova, E.; Bushova, M.; Tenchov, B.; Murata, N. Freezing damage and protective of photosystem 2 by sucrose and trehalose. In *Research Photosynthesis*; Kluwer Academic Publishers: Dordrecht, The Netherlands, 2005; pp. 165–168.
71. Mamedov, M.; Petrova, I.; Yanykin, D.; Zaspas, A.; Semenov, A.Y. Effect of trehalose on oxygen evolution and electron transfer in photosystem 2 complexes. *Biochemistry* **2015**, *80*, 61–66. [[CrossRef](#)]
72. Williams, W.; Gounaris, K. Stabilisation of PS-II-mediated electron transport in oxygen-evolving PS II core preparations by the addition of compatible co-solutes. *Biochim. Biophys. Acta (BBA)—Bioenerg.* **1992**, *1100*, 92–97. [[CrossRef](#)]
73. Mamedov, M.; Nosikova, E.; Vitukhnovskaya, L.; Zaspas, A.; Semenov, A.Y. Influence of the disaccharide trehalose on the oxidizing side of photosystem II. *Photosynthetica* **2018**, *56*, 236–243. [[CrossRef](#)]
74. Francia, F.; Palazzo, G.; Mallardi, A.; Cordone, L.; Venturoli, G. Residual water modulates QA-to-QB electron transfer in bacterial reaction centers embedded in trehalose amorphous matrices. *Biophys. J.* **2003**, *85*, 2760–2775. [[CrossRef](#)]
75. Yanykin, D.; Khorobrykh, A.; Mamedov, M.; Klimov, V. Trehalose stimulation of photoinduced electron transfer and oxygen photoconsumption in Mn-depleted photosystem 2 membrane fragments. *J. Photochem. Photobiol. B Biol.* **2015**, *152*, 279–285. [[CrossRef](#)] [[PubMed](#)]
76. Polander, B.C.; Barry, B.A. A hydrogen-bonding network plays a catalytic role in photosynthetic oxygen evolution. *Proc. Natl. Acad. Sci. USA* **2012**, *109*, 6112–6117. [[CrossRef](#)] [[PubMed](#)]
77. Mamedov, M.D.; Milanovsky, G.E.; Malferrari, M.; Vitukhnovskaya, L.A.; Francia, F.; Semenov, A.Y.; Venturoli, G. Trehalose matrix effects on electron transfer in Mn-depleted protein-pigment complexes of Photosystem II. *Biochim. Biophys. Acta (BBA)—Bioenerg.* **2021**, *1862*, 148413. [[CrossRef](#)] [[PubMed](#)]
78. Ford, R.; Evans, M. Isolation of a photosystem 2 preparation from higher plants with highly enriched oxygen evolution activity. *FEBS Lett.* **1983**, *160*, 159–164. [[CrossRef](#)]
79. Lichtenthaler, H.K. [34] Chlorophylls and carotenoids: Pigments of photosynthetic biomembranes. In *Methods in Enzymology*; Elsevier: Amsterdam, The Netherlands, 1987; Volume 148, pp. 350–382.
80. Ono, T.-A.; Inoue, Y. Mn-preserving extraction of 33-, 24- and 16-kDa proteins from O₂-evolving PS II particles by divalent salt-washing. *FEBS Lett.* **1983**, *164*, 255–260. [[CrossRef](#)]
81. Miyao, M.; Murata, N. Partial disintegration and reconstitution of the photosynthetic oxygen evolution system. Binding of 24 kilodalton and 18 kilodalton polypeptides. *Biochim. Biophys. Acta (BBA)—Bioenerg.* **1983**, *725*, 87–93. [[CrossRef](#)]
82. Klimov, V.V.; Allakhverdiev, S.I.; Shuvalov, V.A.; Krasnovsky, A.A. Effect of extraction and re-addition of manganese on light reactions of photosystem-II preparations. *FEBS Lett.* **1982**, *148*, 307–312. [[CrossRef](#)] [[PubMed](#)]
83. Klimov, V.; Allakhverdiev, S.; Feyziev, Y.M.; Baranov, S. Bicarbonate requirement for the donor side of photosystem II. *FEBS Lett.* **1995**, *363*, 251–255. [[CrossRef](#)]
84. Yanykin, D.V.; Astashev, M.E.; Khorobrykh, A.A.; Pashin, M.O.; Serov, D.A.; Gudkov, S.V. Application of Fixed-Length Ultrasonic Interferometry to Determine the Kinetics of Light-/Heat-Induced Damage to Biological Membranes and Protein Complexes. *Inventions* **2022**, *7*, 87. [[CrossRef](#)]
85. Klimov, V.; Hulsebosch, R.; Allakhverdiev, S.; Wincencjusz, H.; Van Gorkom, H.; Hoff, A. Bicarbonate may be required for ligation of manganese in the oxygen-evolving complex of photosystem II. *Biochemistry* **1997**, *36*, 16277–16281. [[CrossRef](#)]
86. Haldimann, P.; Strasser, R.J. Effects of anaerobiosis as probed by the polyphasic chlorophyll a fluorescence rise kinetic in pea (*Pisum sativum* L.). *Photosynth. Res.* **1999**, *62*, 67–83. [[CrossRef](#)]
87. Redillas, M.C.; Strasser, R.J.; Jeong, J.S.; Kim, Y.S.; Kim, J.-K. The use of JIP test to evaluate drought-tolerance of transgenic rice overexpressing OsNAC10. *Plant Biotechnol. Rep.* **2011**, *5*, 169–175. [[CrossRef](#)]
88. Schansker, G.; Strasser, R.J. Quantification of non-Q B-reducing centers in leaves using a far-red pre-illumination. *Photosynth. Res.* **2005**, *84*, 145–151. [[CrossRef](#)] [[PubMed](#)]
89. Tan, C.-Y.; Huang, Y.-X. Dependence of Refractive Index on Concentration and Temperature in Electrolyte Solution, Polar Solution, Nonpolar Solution, and Protein Solution. *J. Chem. Eng. Data* **2015**, *60*, 2827–2833. [[CrossRef](#)]
90. Anjum, S.A.; Ashraf, U.; Tanveer, M.; Khan, I.; Hussain, S.; Shahzad, B.; Zohaib, A.; Abbas, F.; Saleem, M.F.; Ali, I. Drought induced changes in growth, osmolyte accumulation and antioxidant metabolism of three maize hybrids. *Front. Plant Sci.* **2017**, *8*, 69. [[CrossRef](#)] [[PubMed](#)]
91. Yancey, P. Cellular and molecular physiology of cell volume regulation. In *Competable and Counteracting Solutes*; CRC Press (Taylor & Francis Group): Boca Raton, FL, USA, 1994; pp. 81–110.
92. Ajithkumar, I.P.; Panneerselvam, R. ROS scavenging system, osmotic maintenance, pigment and growth status of *Panicum sumatrense* roth. under drought stress. *Cell Biochem. Biophys.* **2014**, *68*, 587–595. [[CrossRef](#)] [[PubMed](#)]
93. Anjum, N.A.; Aref, I.M.; Duarte, A.C.; Pereira, E.; Ahmad, I.; Iqbal, M. Glutathione and proline can coordinately make plants withstand the joint attack of metal (loid) and salinity stresses. *Front. Plant Sci.* **2014**, *5*, 662. [[CrossRef](#)] [[PubMed](#)]
94. Wang, Y.-M.; Meng, Y.-L.; Nii, N. Changes in glycine betaine and related enzyme contents in *Amaranthus tricolor* under salt stress. *Zhi Wu Sheng Li Yu Fen Zi Sheng Wu Xue Xue Bao—J. Plant Physiol. Mol. Biol.* **2004**, *30*, 496–502.

95. Conde, A.; Silva, P.; Agasse, A.; Conde, C.; Gerós, H. Mannitol transport and mannitol dehydrogenase activities are coordinated in *Olea europaea* under salt and osmotic stresses. *Plant Cell Physiol.* **2011**, *52*, 1766–1775. [[CrossRef](#)]
96. Sharma, S.S.; Dietz, K.-J. The significance of amino acids and amino acid-derived molecules in plant responses and adaptation to heavy metal stress. *J. Exp. Bot.* **2006**, *57*, 711–726. [[CrossRef](#)]
97. Ningthoujam, M.; Habib, K.; Bano, F.; Zutshi, S.; Fatma, T. Exogenous osmolytes suppresses the toxic effects of malathion on *Anabaena variabilis*. *Ecotoxicol. Environ. Saf.* **2013**, *94*, 21–27. [[CrossRef](#)]
98. Bakore, G.; Bararia, M. Kinetics of the Oxidation of D-Glucose by Manganese (III). *Z. Phys. Chem.* **1965**, *229*, 245–249. [[CrossRef](#)]
99. Yanykin, D.V.; Khorobrykh, A.A.; Semenov, A.Y.; Mamedov, M.D. Effect of Trehalose on the Functional Properties of Photosystem II. In *Photosynthesis: Molecular Approaches to Solar Energy Conversion*; Shen, J.-R., Satoh, K., Allakhverdiev, S.I., Eds.; Springer International Publishing: Cham, Switzerland, 2021; pp. 447–464.
100. Judy, E.; Kishore, N. Biological wonders of osmolytes: The need to know more. *Biochem. Anal. Biochem* **2016**, *5*, 1–5. [[CrossRef](#)]
101. Voitsekhovskaja, O.V.; Koroleva, O.A.; Batashev, D.R.; Knop, C.; Tomos, A.D.; Gamalei, Y.V.; Heldt, H.-W.; Lohaus, G. Phloem loading in two Scrophulariaceae species. What can drive symplastic flow via plasmodesmata? *Plant Physiol.* **2006**, *140*, 383–395. [[CrossRef](#)] [[PubMed](#)]
102. Santarius, K.; Milde, H. Sugar compartmentation in frost-hardy and partially dehardened cabbage leaf cells. *Planta* **1977**, *136*, 163–166. [[CrossRef](#)] [[PubMed](#)]
103. Leidreiter, K.; Kruse, A.; Heineke, D.; Robinson, D.; Heldt, H.W. Subcellular volumes and metabolite concentrations in potato (*Solanum tuberosum* cv. Désirée) leaves 1. *Bot. Acta* **1995**, *108*, 439–444. [[CrossRef](#)]
104. Schneider, T.; Keller, F. Raffinose in chloroplasts is synthesized in the cytosol and transported across the chloroplast envelope. *Plant Cell Physiol.* **2009**, *50*, 2174–2182. [[CrossRef](#)] [[PubMed](#)]
105. Wang, C.-T.; Nobel, P.S. Permeability of pea chloroplasts to alcohols and aldoses as measured by reflection coefficients. *Biochim. Biophys. Acta (BBA)—Biomembr.* **1971**, *241*, 200–212. [[CrossRef](#)]
106. Schäfer, G.; Heber, U. Glucose transport into spinach chloroplasts. *Plant Physiol.* **1977**, *60*, 286–289. [[CrossRef](#)]
107. Nägele, T.; Heyer, A.G. Approximating subcellular organisation of carbohydrate metabolism during cold acclimation in different natural accessions of *Arabidopsis thaliana*. *New Phytol.* **2013**, *198*, 777–787. [[CrossRef](#)]
108. Patzke, K.; Prananingrum, P.; Klemens, P.A.W.; Trentmann, O.; Rodrigues, C.M.; Keller, I.; Fernie, A.R.; Geigenberger, P.; Bölder, B.; Lehmann, M.; et al. The Plastidic Sugar Transporter pSuT Influences Flowering and Affects Cold Responses. *Plant Physiol.* **2019**, *179*, 569–587. [[CrossRef](#)]

Disclaimer/Publisher’s Note: The statements, opinions and data contained in all publications are solely those of the individual author(s) and contributor(s) and not of MDPI and/or the editor(s). MDPI and/or the editor(s) disclaim responsibility for any injury to people or property resulting from any ideas, methods, instructions or products referred to in the content.